International Journal of Engineering Trends and Technology
ISSN: 2231–5381 / https://doi.org/10.14445/22315381/IJETT-V73I1P105

Volume 73 Issue 1, 68-76, January 2025

Original Article

A First Principle Analysis of Electrical and Superconducting Properties of $YBa_2Cu_3O_7$

Laxmikanta Mahapatra[1], Gyanananda Panda[1], Kamal Lochan Mohanta[1*]

[1]*Department of Physics, ITER, Siksha 'O' Anusandhan (Deemed to Be University), Bhubaneswar, Odisha, India.*

[*]*Corresponding Author : kamalmohanta@soa.ac.in*

Received: 24 May 2024 Revised: 11 December 2024 Accepted:27 December 2024 Published: 31 January 2025

Abstract *- The compound $YBa_2Cu_3O_7$ (Y-123) was discovered in 1987. It is a Cu-based high-Tc superconducting compound with a Perovskite-like structure. It was the first material that showed its superconducting character above the temperature of Liquid Nitrogen, i.e. at 77K. We have calculated the electronic properties of $YBa_2Cu_3O_7$ using Quantum ESPRESSO with the DFT approach. By modifying this material's lattice parameter and other geometrical properties, we obtained its SCF (Self-Consistent Field), calculated the Density of States (DOS), energy band structure, pressure effect, and Fermi surface, and described it more widely. We observed decreased transition temperature, lattice parameter, and unit cell volume by applying pressure from 1GPa to 15GPa. Here, we have used CASTEP software to calculate the Fermi surface of the material $YBa_2Cu_3O_7$.*

Keywords *- First principle calculation, Density functional theory, Band diagram, Density of states, Pressure effect.*

1. Introduction

Superconductors can conduct electricity with zero resistance [1, 2] and with no supply availability, and superconductors' electrons respond differently than metals at tiny levels [3]. As High Temperature Superconductors (HTS) have the potential to revolutionize the advancement of magnetic incarceration union by allowing high current to be passed under high fields at preferential temperatures occasioning in tinier reactors with lower assets costs [4, 5] and the peculiar milieu of a meld reactor. In contrast, it creates hurdles that demand additional attention. It was started in 1986 when George Bednorz and Karl Alex Muller discovered the first cuprate superconducting compound (Lanthanum-Barium-Copper-oxide) [6]. Following this, Maw-Kuen-Wu and Chu-Ching-Wu discovered the Yttrium-Barium-Copper-Oxide (Y-123) compound very next year [7]. In material science, research has been done on the crystal structure of YBCO superconductors, which has greatly captivated me. Researchers are currently developing superconducting materials with a higher critical temperature, and the Y–Ba–Cu–O system can superconductivity at temperatures of 155K or higher [8]. However, this system is exceedingly unstable if it cannot be synthesized [9]. Researchers have also put much effort into figuring out the essential features required in determining superconductivity, and it was discovered that a better understanding of electronic evolution will aid in formulating the critical physical reasons that lead to superconductivity [10]. So, evaluating the electronic properties of various superconducting materials is vital. But in this paperwork, we have given more emphasis on copper-based superconductors out of all types of superconductors; particularly, our focus is on YBa2Cu3O7 [Y-123] ceramic compound, which is a family of high temperature copper-based superconductor [6], consisting of copper oxide (CuO2) layers with alternating ion-containing layers, i.e. Lanthanum, Barium, and Strontium which operate as charge reservoirs. Here, the oxygen content of the CuO chain is thought to control the concentration of holes in the CuO2 planes [8, 11]. In the CuO2 layer, it is observed that cooper pair formation takes place and electrical current flows inside it, and they are stored in ion containing layers afterwards and exhibit the superconducting property for which YBa2Cu3O7 crystal or model is also termed as charge transfer model [7, 12].

Here, the matter of concern is on BCS theory, which explains the superconductivity property of materials not in a prescribed manner, while pairing mechanisms do that to some extent [13]. In this Y-123 compound the individual atoms configuration is characterized as [(Y3+)(Ba2+)2(Cu3+)(Cu2+)2(O2-)7]. So, copper ions with +2 and +3 charges are arranged in a check-board pattern that resembles a perovskite-like structure. So, charge ordering [14] is the term coined for this phenomenon. Further, it clarifies that the superconducting phenomenon is due to the Cu+3 ion [15], and the presence of the cu2+ ion suggests that the electron-phonon interaction is less prominent in the Y-123 compound. And all this property of the Y-123 compound occurs at the transition temperature Tc = 93K [16]. Here, the oxygen gist inside the CuO chains also influences the transition temperature of the YBa2Cu3O7 superconductor.

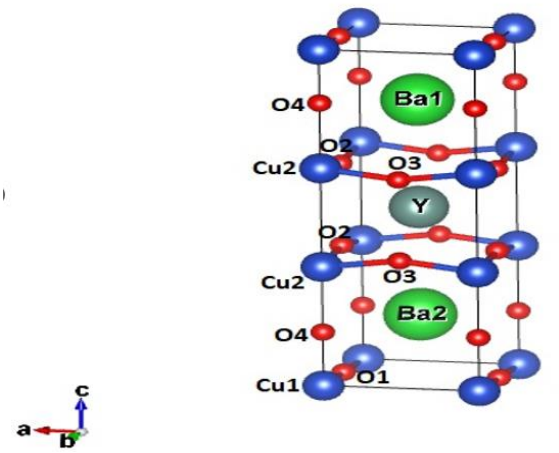

Fig. 1 Crystal structure of $YBa_2Cu_3O_7$

With diminishing oxygen matter, the transition temperature (Tc) declines [17]. On the other hand, most of these studies concentrate on the character of both energy bands and state densities near the Fermi level rather than providing much more numerical information about the charge distributions. Results of these computations demonstrate a fair amount of consistency in terms of general characteristics such as (i) Significant two-dimensional characteristics of the bands being roughly linear along the Γ-Z direction, (ii) and almost several strips (bands) are half-occupied. (iii) the Cu-d and O-p orbitals are solely responsible for these half-filled bands (iv). Compared with conventional superconductors, the Fermi-level density of states is minimal [18]. This draws our attention again to studying their electrical features and physical properties more descriptively. The proceeding section of this paper contains the computational approach, structure, results and their description, effect of pressure, Fermi surface, conclusion, acknowledgement and references, respectively.

2. Computational Approach

We know that DFT (Density Functional Theory) is a beneficial baseline tool for exploring the variations within the comparable configurations and their consequences on the superconducting phase, and the relevance of this paradigm to cuprate superconductivity was validated just after a practical survey demonstrated remarkable match with the computed evaluations. Here, the most basic elements of heavily interrelated models, such as Hubbard U, hopping integrals, carrier density, and so on, may be calculated by employing DFT as a preliminary step before executing a firmly associated computation. So here, the Quantum-ESPRESSO package [16] of DFT is used to calculate all of the first principle computations of this study. Here, the plane wave pseudo-potential approach is used to solve the Kohn–Sham equations (non-interacting fermions have a Schrodinger-like equation that creates the same density as interacting entities do with respective systems). The projector augmented-wave function [(PAW) = hybrid of pseudopotential + linear augmented wave function] approach is used to characterize the interactions, including valence electrons and the ion hub [19]. The electronic exchange-correlation verve was outlined using Perdew-Bruke-Ernzerhof (PBE) sort of the GGA (Generalized Gradient Approximation) [20] and here we have taken orthorhombic structure with lattice parameter (a, b, c) as (3.845, 3.926, 11.824 A^0) respectively to perform the DFT calculation. Pslibrary 1.0.0 [21] provided the pseudopotentials for the elements Y, Ba, Cu and O, and because of its easy response, we used the norm-conserving pseudopotential method throughout the calculation [22]. Here cut-off wave-function and charge-density of (30, 300) Ry picked accordingly to examine the Brillouin zone (BZ), and we implemented the Monkhorst-Pack strategy of [3 x 3 x 1] K-mesh here [23] and the two-body potential function [24] is used to model the interactions between the atoms in bulk ($YBa_2Cu_3O_7$).

3. Structure

The first step in understanding the physical properties of any material is to comprehend its structural information. Here, Figure 1 depicts the $YBa_2Cu_3O_7$ ceramic compound, which has an orthorhombic (pmmm, space group) [25] construction, and by considering a single unit cell, we can see that it is comprised of three planes that are arranged serially as Cu (1)O(1) plane, BaO plane and CuO_2 plane. The two Cu atom planes having charges of (3+ and 2+) [26] are distinguished from one another by the BaO plane (charge reservoir plane), while the Y atom isolates the two conjugative CuO_2 planes [3]. The Cu (1)O(1) plane looks ribbon-shaped, whereas the CuO_2 plane resembles a square planner's layout.

Here, the hole intensity in the CuO_2 flat surface is extensively used by model parameters at theoretical superconducting concepts, and the correlation between the two CuO_2 layers, as well as among the CuO_2 and BaO layers, is very weak here. Simultaneously the lower fluctuation of $d_{Cu(1)-O(4)}$ suggests potent Cu(1)-O(4) interactions [12]. In this bulk, there are 4 types (a total of 13 atoms) situated in this primitive cell. 8 out of 13 atoms are inequivalent here, and we have introduced two vacant spheres in this crystal that fix the cavities in geometry. One is in the Y-layer to replace the defective oxygen atom, and another is in the Cu-O plane to fill in the porosity in the structure [18]. The atomic configuration of all 13 atoms of the Y-123 compound has been shown in the Table 1.

Generally, this Y-123 compound is a stoichiometry compound with an X value of 0 in oxygen content of $YBa_2Cu_3O_{7-x}$ configuration. If the X value decreases from 7, i.e. if the value of X= 1, then this Stoichiometry Y-123 material [27, 28] undergoes transformation and changes to a non-stoichiometry compound where the O(1) site of the Cu(1) layer remains vacant giving rise to tetragonal orientation.

Table 1. Atomic positions of $YBa_2Cu_3O_7$ Crystal in A^0

Atom	Position of a	Position of b	Position of c
Ba	1.922334	1.963076	9.688204
Ba	1.922334	1.963076	2.13546
Y	1.922334	1.963076	5.911832
Cu	0.000000	0.000000	7.646103
Cu	0.000000	0.000000	4.177561
Cu	0.000000	0.000000	0.000000
O	0.000000	1.963076	0.000000
O	1.922334	0.000000	7.338393
O	1.922334	0.000000	4.485271
O	0.000000	1.963076	7.350193
O	0.000000	1.963076	4.473471
O	0.000000	0.000000	9.941573
O	0.000000	0.000000	1.882091

4. Results and Discussion

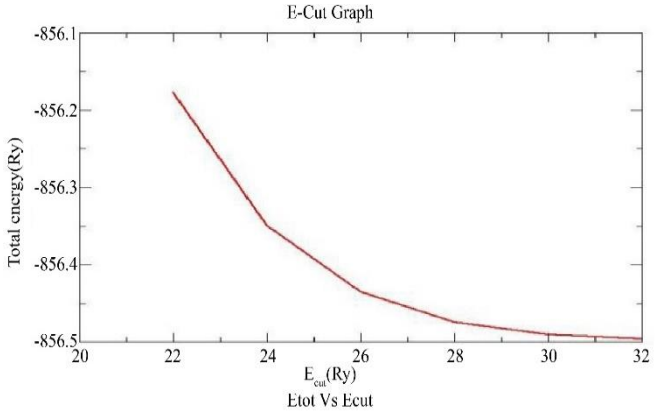

Fig. 2 Convergence test of plane wave cutoff (E_{cut}) in Ry

In order to minimize the error percentile of the lattice parameter, we took the calculation and description of the electronic feature of the ceramic compound $YBa_2Cu_3O_7$. We first have to optimize it, and then we have to converge it. So, for convergence of the lattice parameter, we have to perform the convergence test, which is performed by showing a graphical method through comparison among the total energy value along the Y-axis and the cut-off energy value along the X-axis, as shown in Figure 2. From Figure 2, we can examine that with the increase of cut-off energy value, the total energy value gradually decreases and converge at a value around 30Ry and as acknowledged here all energy scales are taken in atomic Rydberg (Ry) units. In this, spherical symmetry is assumed for the charge densities and potentials. Only the valence electron charge density is reevaluated during the repetitions [18]. Similarly, the convergence test of Brillouin Zone (BZ) is done by sampling method by taking the k-points at the X-axis and total energy at the Y-axis and found that the total energy value decreases with the corresponding increase in value of the k-point and finally converge at the value of k-mesh to be [3 x 3 x 1] which will be most suitable for our calculation.

So, considering the above, we have taken the cutoff plane wave function at 30Ry and k-mesh at [3 x 3 x 1]. Here, the occupation of smearing methfessel-paxton type with a smearing width of 0.02Ry to perform the standard Self Consistent Field (SCF) settings is calculated. In our calculation, the convergence threshold on total energy is taken as $10^{-6,}$ and the starting point of charge density and wave function are arranged in [atomic, atomic + random] fashion. Similarly, spin polarization is taken in a collinear fashion for magnetization, and the value of starting atomic magnetization of Y, Ba, Cu and O are taken at 0.2000, 0.0000, 0.2000, and 0.0000, respectively.

4.1. Band Diagram

Although several bands in the valence band area are substantially hybridized, the band diagram around the Fermi stage may also be interpreted in basic expressions. Only four bands go across the Fermi level [29], and we have also found the same phenomena in Figure 3 at high symmetry points. Here, Cu-d and O-p orbitals produce 36 bands in the valence band. Two sets of narrow bands develop from O-2s and Ba-5p orbitals underneath the valence band, which are permitted to soften over iteration [30]. The antibonding mixture of Cu-d and O-p orbitals of two CuO_2-planes gives rise to Bands 1 and 2. Near the foot of the valence band, the bonding pair of bands occurs because the yttrium layer effectually separates the Cu-O-layers and hence decreases the action involved between them. So, these two bands have practically degenerate behaviour. Here, almost the two bands are half-empty and half-filled, where one is a little less than half-filled and the other somewhat more than half-filled. This results in a substantial nesting of the Fermi surface's corresponding sheets. Here, the CuO chains are responsible for the second set of bands, i.e. numbers 3 and 4. Band number 3 in the above figure displays the substantial dispersion in the Γ-Y and X-S axes and is almost smooth in the other two ways. This is strong evidence of the band's fundamentally one-dimensional nature. Its dispersion is similar to the two bands stated above along the X-S axis.

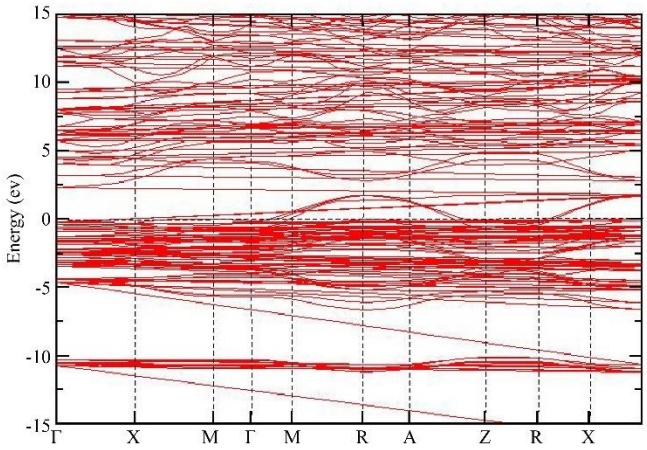

Fig. 3 Band diagram of $YBa_2Cu_3O_7$ compound

So, two inferences may be derived from this: First, the Ba-O plane separates the chain from Cu-O-planes, and the little pockets encircling the S point have the major share of the BaO plane's characteristics. Second, the binding among Cu and O-atoms in the chain and planes is nearly similar. Here, Cu-d and O-p orbitals of the chain-atoms produce an antibonding combination that forms this band. Unlike the previous pair, one band is practically vacant while the other is full, and here, the Cu (1) d-band is around 30% broader than the Cu (2) d-band, which is a remarkable property observed and the widths of the oxygen p-band do not vary much here [18].

4.2. Density of States

The degree of states accessible to electrons for every energy interval across each energy level is termed the Density of States (DOS). Figure 5 depicts the partial densities of states in Cu-d and O-p orbitals and the total density of states at various locations. Here, we have demonstrated the density of states (DOS) in Figure 4 by applying the tetrahedron occupation and broadening. Also, we have taken the k-mesh value [6 x 6 x 2] and observed that the CuO_2 plane masters the density of states near the Fermi layer, demonstrating that the CuO_2 plane is the major conductivity controller in this crystal.

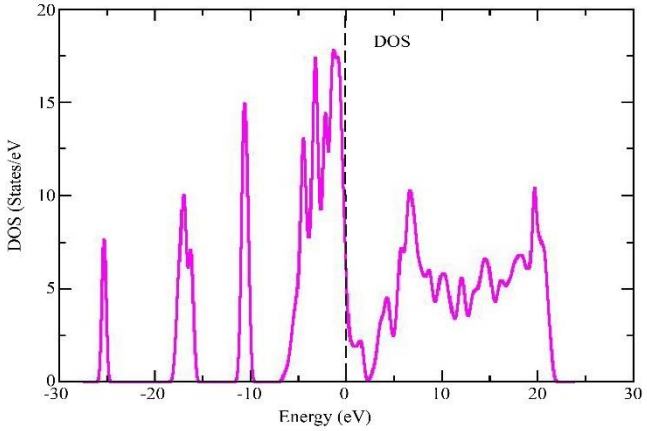

Fig. 4 Density of states of $YBa_2Cu_3O_7$ compound

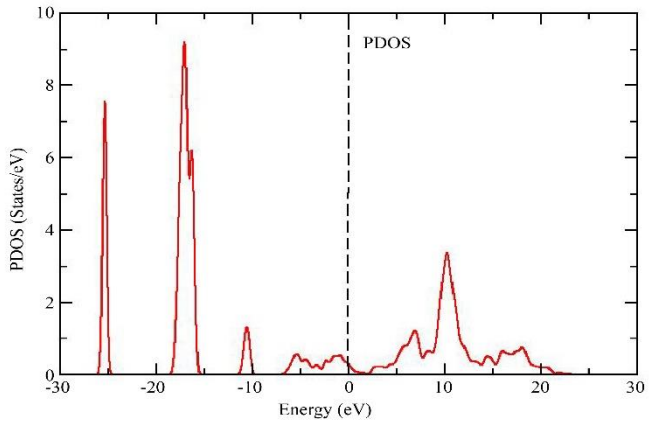

Fig. 5 Partial density of states of $YBa_2Cu_3O_7$ compound

Here, the contributions of Ba and Y in the partial density of state are extremely low and unnoticed in our consultation. We have been associated with states that may arise from planes or chains in these several peaks. The planes dominate the states right above the Fermi level. Meanwhile, the chain governs the top of the valence band. Here, the peak shows the plane characteristics. We see two strong peaks at (A) and (B), which characterize the (P-DOS) of the apical oxygen O-(4). These peaks have a prominent Cu(1)-d and Cu(2)-d character, hinting that they are linked to the bond that holds the layers jointly, and it also gives information about the hybridization between the BaO plane and the CuO chain which is much greater than the hybridization of the CuO_2 plane and the BaO chain suggesting intense covalent bonds between Cu(1) and O(4) as well as Cu(2)-O(4) and no covalent bond between the two CuO_2 planes at no pressurize condition [18].

4.3. Pressure Effect on YBa_2Cu_3O7

Researchers have widely studied the effects of pressure on high-Tc cuprates. Almost all the reported high-pressure measurements have centered on the unconventional variation of superconducting critical temperature (Tc) with pressure. Enforcing pressure is close to enhancing doping levels by redistributing carriers. In the case of $YBa_2Cu_3O_7$ a possible mechanism for carrier redistribution involves charge transfer from the CuO chains to the CuO_2 planes [31]. Naturally, pressure can influence the electronic dimensionality by compressing the lattice.

Discovering how pressure impacts the quasi-two-dimensional state is intriguing, a characteristic of high-Tc superconductors often depicted as carrier confinement with CuO_2 planes. Our work examines the pressure dependence of resistivity and Hall coefficient in untwined single crystals of $YBa_2Cu_3O_7$ under hydrostatic pressure up to 15 GPa, targeting to uncover the underlying physics behind the pressure effects in high-Tc cuprates. Generally, superconductors are not found at room temperature. This is the biggest difficulty in practical application.

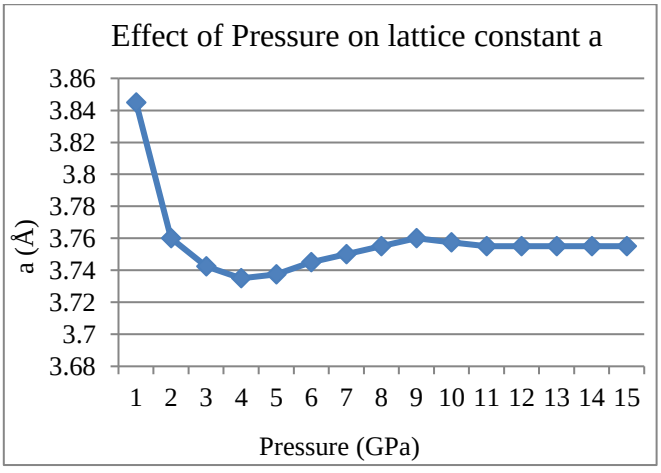

Fig. 6 Lattice constant a verses pressure for $YBa_2Cu_3O_7$ superconductor

To resolve this problem, many researchers have developed superconducting materials at room temperature by applying high pressure. Under high pressure (267±10 GPa), the Ceous sulfur hydride shows superconductivity at room temperature. This gives hope that it will work under high pressure to produce superconductivity materials at room temperature. Here, we are interested in knowing the effect of pressure, i.e., how pressure affects the $YBa_2Cu_3O_7$. Here, by applying a pressure in between the range from 1 GPa to 15 GPa in Quantum ESPRESSO to plot graphs between pressure vs. lattice constants a, b, c in A^0, pressure vs. b/a ratio, pressure vs. c/a ratio, pressure vs. volume, pressure vs. V/V0. From figures (Figures 6 to 12), we found that the transition temperature decreased due to high pressure, and at a certain point of pressure, the superconducting transition temperature slowly increased. The crystallographic phase or electrical arrangement may change by applying pressure. We observed that applying pressure decreased the lattice parameters and unit cell volume. This indicates that the apparent density of $YBa_2Cu_3O_7$ increases with increasing pressure. An increase in pressure results in reduced spacing between the atoms.

Table 2. Calculated values of lattice constants, variations, and volume for $YBa_2Cu_3O_7$ up to 15GPa

Pressure (GPa)	a (A^0)	b (A^0)	c (A^0)	c/a	a*b*c (Cubic A^0)	b/a	v/v0
1	3.845	3.926	11.825	3.075423	178.5039	1.021066	1.000084
2	3.76	3.847	11.59	3.082447	167.6461	1.023138	0.939252
3	3.7425	3.835	11.52	3.078156	165.3407	1.024716	0.926335
4	3.735	3.84	11.47	3.07095	164.5073	1.028112	0.921666
5	3.7375	3.85	11.42	3.055518	164.3267	1.0301	0.920654
6	3.745	3.858	11.385	3.040053	164.4929	1.030174	0.921585
7	3.75	3.857	11.375	3.033333	164.5252	1.028533	0.921766
8	3.755	3.855	11.3725	3.028628	164.6229	1.026631	0.922314
9	3.76	3.854	11.37	3.023936	164.7631	1.025	0.9231
10	3.7575	3.854	11.372	3.02648	164.6825	1.025682	0.922648
11	3.755	3.854	11.373	3.028762	164.5874	1.026365	0.922115
12	3.755	3.8545	11.374	3.029028	164.6233	1.026498	0.922316
13	3.755	3.855	11.375	3.029294	164.6591	1.026631	0.922517
14	3.755	3.855	11.37	3.027963	164.5867	1.026631	0.922111
15	3.755	3.855	11.37	3.027963	164.5867	1.026631	0.922111

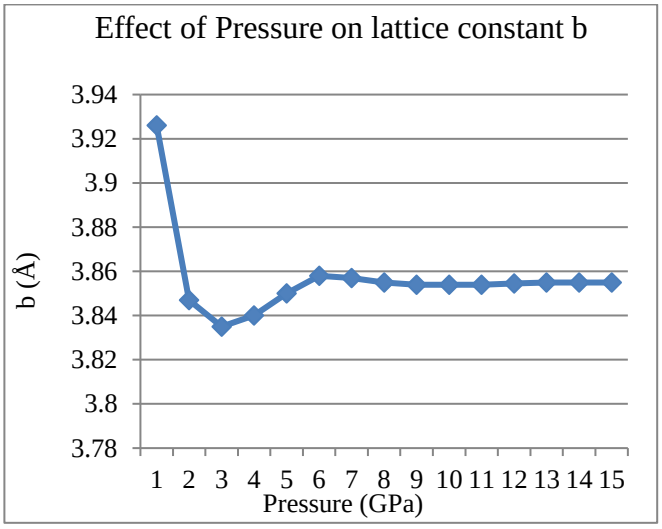

Fig. 7 Lattice constant b versus Pressure for $YBa_2Cu_3O_7$ superconductor

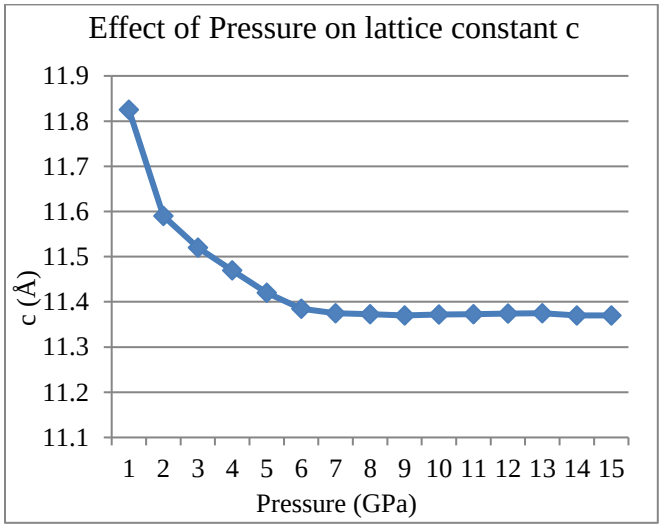

Fig. 8 Lattice constant c versus Pressure for $YBa_2Cu_3O_7$ superconductor

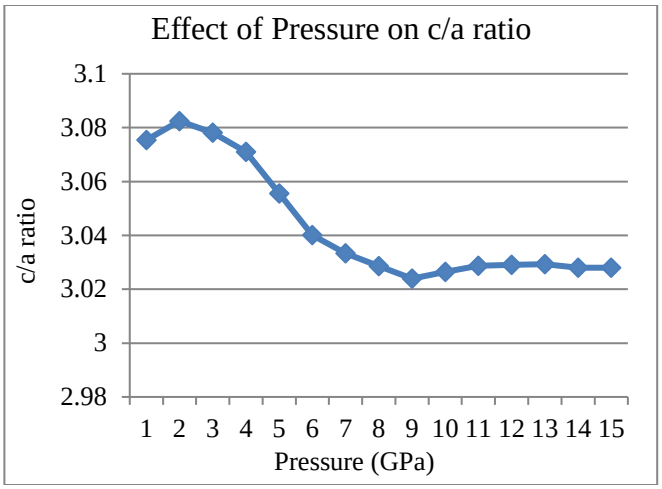

Fig. 9 Lattice constant c/a versus Pressure for $YBa_2Cu_3O_7$ superconductor

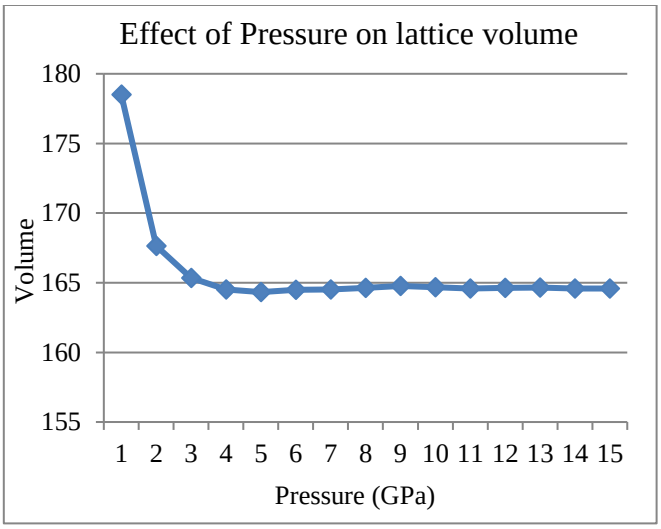

Fig. 11 Volume versus Pressure for $YBa_2Cu_3O_7$ superconductor

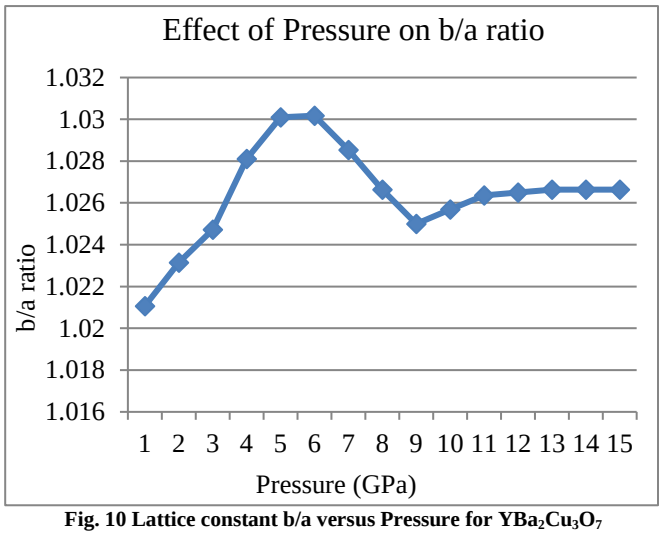

Fig. 10 Lattice constant b/a versus Pressure for $YBa_2Cu_3O_7$ superconductor

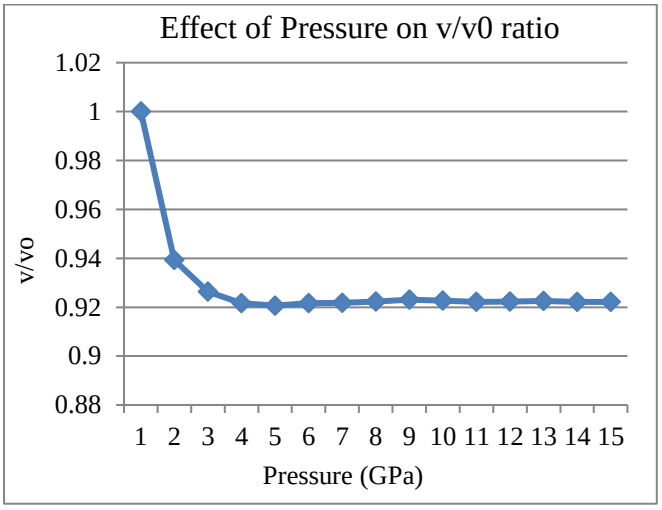

Fig. 12 v/v0 verses Pressure for $YBa_2Cu_3O_7$ superconductor

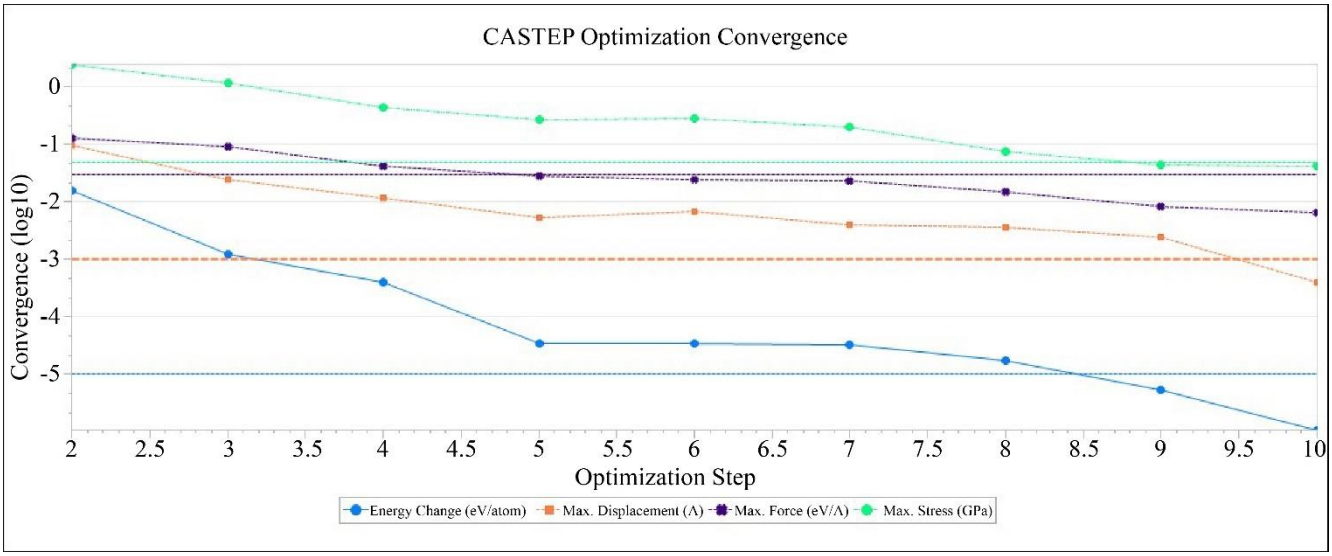

Fig. 13 Optimization step Vs. Convergence (log 10)

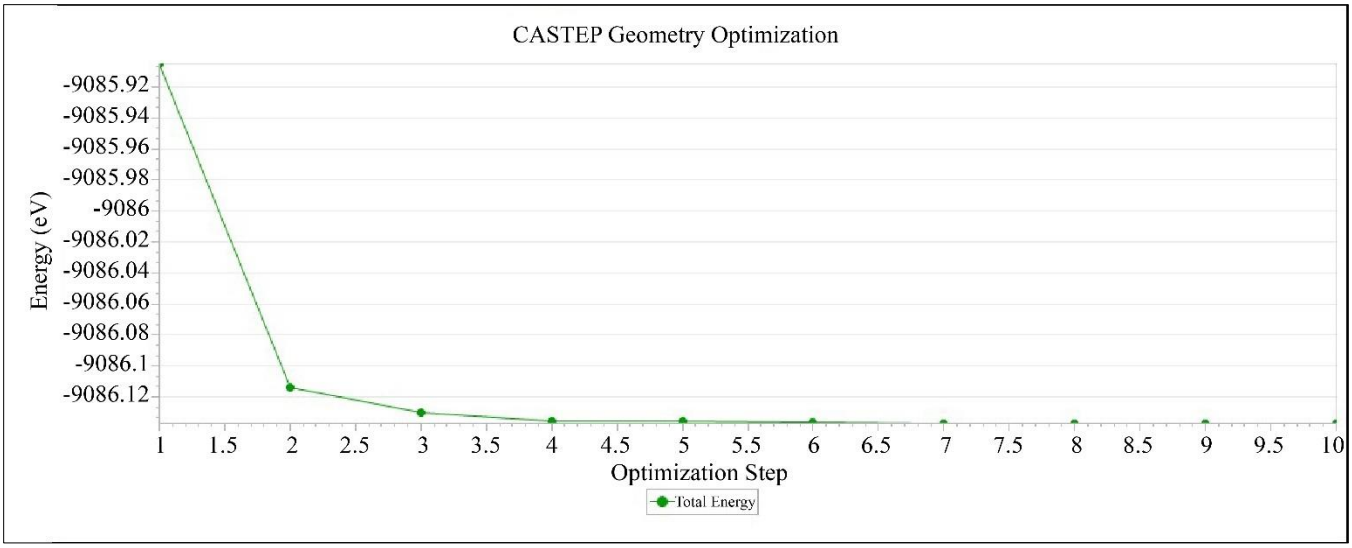

Fig. 14 Optimization step Vs. Energy (eV)

4.4. Fermi Surface

The Fermi surface is fundamental in studying metals and their electronic properties. The structure of a Fermi surface is vital in deciding the rate of nesting in materials, which in turn enhances magnetic and orbital ordering. It is defined as the set of all possible states that electrons can occupy at the Fermi energy, which is the highest energy level and is occupied at absolute zero temperature. The face of the metal is also called the Fermi surface because it determines many physical phenomena that depend on the interaction of the electrons with external fields, such as electrical conductivity, magnetism, superconductivity and thermoelectricity. The shape and topology of the Fermi surface can vary widely depending on the type and arrangement of atoms in the metal and can reveal important information about the underlying crystal structure and symmetry. We used a software tool named Cambridge Serial Total Energy Package (CASTEP) [32, 33] that can visualize various properties related to the Fermi surface of any material based on its K-dependence. This program allows us to explore and analyze different materials' electronic structures and transport phenomena interactively and intuitively.

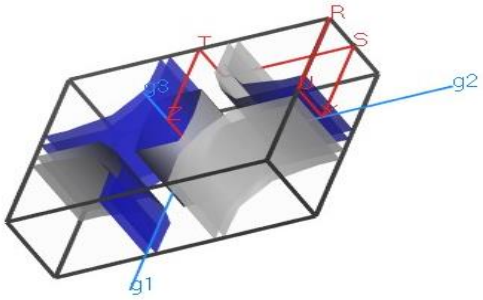

Fig. 15(b)

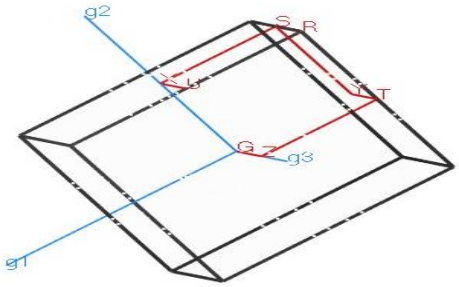

Fig. 15(c)

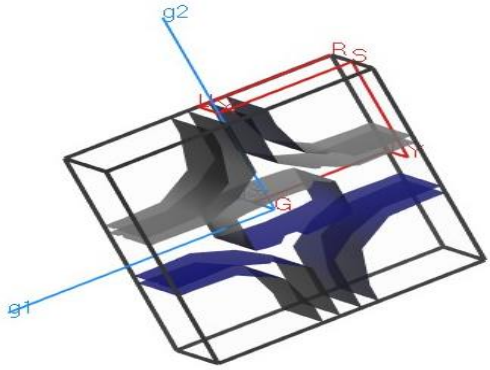

Fig. 15(a)

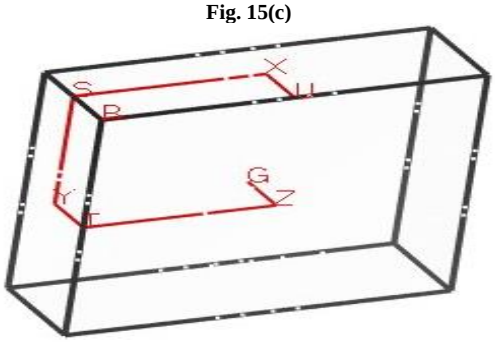

Fig. 15(d)

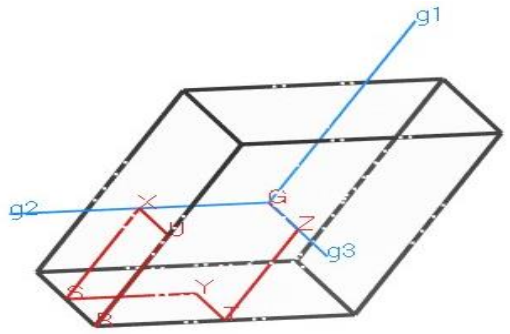

Fig. 15(e)
Fig. 15(a) - 15(e) represent fermi surface

Figures 13 and 14 represent the CASTEP optimization convergence and CASTEP geometry optimization of $YBa_2Cu_3O_7$. The Fermi surface figures (Figure 15 (a)-15(e)) of the superconducting material $YBa_2Cu_3O_7$ are given below. Here, g_1, g_2 and g_3 represent the coordinate axes.

5. Conclusion

In this study, we used the DFT approach to illustrate the electrical characteristics of the $YBa_2Cu_3O_7$ crystal. The PBE variant of the GGA was used to calculate the electronic exchange co-relation energy. The band gap energies total and partial density of states have all been resolved. O_2 concentration in CuO chains determines the transition temperature of the $YBa_2Cu_3O_7$ superconductor, i.e. with decreasing oxygen saturation, the transition temperature Tc drops.

The charge transfer followed a layered pattern, with the Cu-O-chains and B-layers losing electrons to the Cu-O-planes and Y-layers. Based on the mechanical and dynamic stability evaluations, we also confirm that the orthorhombic configuration stays secure here, and no structural phase change occurs under pressure conditions. Again, based on the charge transfer model, the growth of charge density at the CuO_2 plane can also represent qualitative adjustment in the superconducting effect. So, within a BCS picture, the BCS picture of the superconductivity procedure is still favoured when investigating the superconductivity of cuprates.

Acknowledgement

The authors sincerely appreciate the Institute of Physics (IOP) in Bhubaneswar (India) for incorporating a centre of excellence.

References

[1] Michel Van Camp, O. Francis, and T. Lecocq, "Recording Belgium's Gravitational History," *Eos*, 2017. [CrossRef] [Google Scholar] [Publisher Link]

[2] Michel Van Camp et al., "Geophysics from Terrestrial Time-Variable Gravity Measurements," *Reviews of Geophysics*, vol. 55, no. 4, pp. 938-992, 2017. [CrossRef] [Google Scholar] [Publisher Link]

[3] Jin-Jin Cao, Tian-Ge Wang, and Xiao-Fan Gou, "Predictions for Structural Stability and Electronic Evolution in Pressure-Induced Overdoped $YBa_2Cu_3O_7$," *Computational Material Science*, vol. 155, pp. 416-423, 2018. [CrossRef] [Google Scholar] [Publisher Link]

[4] A. Sykes et al., "Compact Fusion Energy Based on the Spherical Tokamak," *Nuclear Fusion*, vol. 58, no. 1, pp. 1-9, 2017. [CrossRef] [Google Scholar] [Publisher Link]

[5] Alan Sykes et al., "Recent Advances on the Spherical Tokamak Route to Fusion Power," *IEEE Transactions on Plasma Science*, vol. 42, no. 3, pp. 482-488, 2014. [CrossRef] [Google Scholar] [Publisher Link]

[6] J.G. Bednorz, and K.A. Müller, "Possible High T_c Superconductivity in the Ba−La−Cu−O System," *Journal of Physics B Condensed Matter*, vol. 64, pp. 189-193, 1986. [CrossRef] [Google Scholar] [Publisher Link]

[7] J.L. Tallon et al., "Generic Superconducting Phase Behavior in High-T_c Cuprates: T_c Variation with Hole Concentration in YBa2Cu3O7$_{-\delta}$," *Physical Review B*, vol. 51, no. 18, pp. 12911-12914, 1995. [CrossRef] [Google Scholar] [Publisher Link]

[8] S.R. Ovshinsky et al., "Superconductivity at 155 K," *Physical Review Letters*, vol. 58, no. 24, pp. 2579-2581, 1987. [CrossRef] [Google Scholar] [Publisher Link]

[9] Ismail Yucil, and Seyfettin Cakmak, "The Role of Carbon (C) Atoms on YBCO Superconductor: DFTstudy," *Optoelectronics and Advanced Materials-Rapid Communications*, vol. 11, no. 9-10, pp. 590-599, 2017. [Google Scholar]

[10] P.L. Alireza et al., "Accessing the Entire Overdoped Regime in Pristine $YBa_2Cu_3O_{6+x}$ by Application of Pressure," *Physical Review B*, vol. 95, no. 10, 2017. [CrossRef] [Google Scholar] [Publisher Link]

[11] Guo-Zheng Li, Xiang-Yun Deng, and Lei Dong, "Facile Fabrication of Nano-Composited Y-Ba-Cu-O Single-Grain Superconductor using Raw Metallic Oxides," *Materials Chemistry and Physics*, vol. 167, pp. 14-17, 2015. [CrossRef] [Google Scholar] [Publisher Link]

[12] Rainer Wesche, *Physical Properties of High Temperature Superconductors*, Wiley, pp. 1-544, 2015. [Google Scholar] [Publisher Link]

[13] J.G. Storey, J.L. Tallon, and G.V.M. Williams, "Saddle-Point Van Hove Singularity and the Phase Diagram of High-T_c Cuprates," *Physical Review B*, vol. 76, no. 17, 2007. [CrossRef] [Google Scholar] [Publisher Link]

[14] W.J. Padilla et al., "Constant Effective Mass across the Phase Diagram of High-T_c Cuprates," *Physical Review B*, vol. 72, no. 6, 2005. [CrossRef] [Google Scholar] [Publisher Link]

[15] M.K. Wu et al., "Superconductivity at 93 K in a New Mixed-Phase Y-Ba-Cu-O Compound System at Ambient Pressure," *Physical Review Letters*, vol. 58, no. 9, pp. 908-910, 1987. [CrossRef] [Google Scholar] [Publisher Link]

[16] P Giannozzi et al., "Advanced Capabilities for Materials Modelling with Quantum ESPRESSO," *Journal of Physics: Condensed Matter*, vol. 29, no. 46, 2017. [CrossRef] [Google Scholar] [Publisher Link]

[17] K. Larbaoui et al., "Effect of Oxygen Deficiencies and the Substitution of Fluorine on the Electronic States in $YBa_2Cu_3O_{7\mp\delta}$ Superconductors," *Journal of Alloys and Compounds*, vol. 414, no. 1-2, pp. 20-25, 2006. [CrossRef] [Google Scholar] [Publisher Link]

[18] R. Pankaluoto, and K. Kaski, "Electronic Structure Study of Y-Ba-Cu-O High Temperature Superconductor," *Physica Scripta*, vol. T33, pp. 227-234, 1990. [Google Scholar] [Publisher Link]

[19] G. Kresse, and D. Joubert, "From Ultrasoft Pseudopotentials to the Projector Augmented-Wave Method," *Physical Review B*, vol. 59, no. 3, pp. 1758-1775, 1999. [CrossRef] [Google Scholar] [Publisher Link]

[20] John P. Perdew, Kieron Burke, and Matthias Ernzerhof, "Generalized Gradient Approximation Made Simple," *Physical Review Letters*, vol. 77, no. 18, pp. 3865-3868, 1996. [CrossRef] [Google Scholar] [Publisher Link]

[21] Andrea Dal Corso, "Pseudopotentials Periodic Table: From H to Pu," *Computational Materials Science*, vol. 95, pp. 337-350, 2014. [CrossRef] [Google Scholar] [Publisher Link]

[22] D.R. Hamann, M. Schlüter, and C. Chiang, "Norm-Conserving Pseudopotentials," *Physical Review Letters*, vol. 43, pp. 1494-1497, 1979. [CrossRef] [Google Scholar] [Publisher Link]

[23] Hendrik J. Monkhorst, and James D. Pack, "Special Points for Brillouin-Zone Integrations," *Physical Review B*, vol. 13, 1976. [CrossRef] [Google Scholar] [Publisher Link]

[24] S.L. Chaplot, "Interatomic Potential, Phonon Spectrum, and Molecular-Dynamics Simulation up to 1300 K in YBa2Cu3O7$_{-\delta}$," *Physical Review B*, vol. 42, 1990. [CrossRef] [Google Scholar] [Publisher Link]

[25] Samuel T Murphy, "A Point Defect Model for $YBa_2Cu_3O_7$ from Density Functional Theory," *Journal of Physics Communications*, vol. 4, no. 11, pp. 1-15, 2020. [CrossRef] [Google Scholar] [Publisher Link]

[26] L.A. Curtiss, T.O. Brun, and D.M. Gruen, "Valence Fluctuations in the (Yttrium Barium Copper Oxide), YBa2Cu3O7-x Superconductor," *Inorganic Chemistry*, vol. 27, no. 8, pp. 1421-1425, 1988. [CrossRef] [Google Scholar] [Publisher Link]

[27] B. Prabhakar, and Tanveer Ahmad Wani, "Mechanical Properties of YBCO Superconductor under High-Pressure," *Indian Journal of Science and Technology*, vol. 13, no. 22, pp. 2264-2271, 2020. [CrossRef] [Google Scholar] [Publisher Link]

[28] R.J. Cava et al., "Oxygen Stoichiometry, Superconductivity and Normal State Properties of YBa2Cu3O7−δ," *Nature*, vol. 329, pp. 423-425 ,1987. [CrossRef] [Google Scholar] [Publisher Link]

[29] Jaejun Yu et al., "Bonds, Bands, Charge Transfer Excitations and Superconductivity of $YBa_2Cu_3O_{7-\delta}$," *Physics Letters A*, vol. 122, no. 3-4, pp. 203-208, 1987. [CrossRef] [Google Scholar] [Publisher Link]

[30] S. Massidda et al., "Electronic Structure and Properties of $YBa_2Cu_3O_{7-\delta}$, a Low Dimensional, Low Density of States Superconductor," *Physics Letters A*, vol. 122, no. 3-4, pp. 198-202, 1987. [CrossRef] [Google Scholar] [Publisher Link]

[31] Budigi Prabhakar, and Tanveer Ahmad Wani, "First Principle Energy Calculation of YBCO Superconductor," *Indian Journal of Science and Technology*, vol. 13, no. 33, pp. 3425-3429, 2020. [CrossRef] [Google Scholar] [Publisher Link]

[32] Stewart J. Clark et al., "First Principles Methods Using CASTEP," *Journal of Crystallography - Crystalline Materials*, vol. 220, pp. 567-570, 2009. [CrossRef] [Google Scholar] [Publisher Link]

[33] M.D. Segall et al., "First -Principles Simulation: Ideas, Illustrations and the CASTEP Code," *Journal of Physics: Condensed Matter*, vol. 4, no. 11, pp. 2717-2744, 2002. [CrossRef] [Google Scholar] [Publisher Link]